Development of Reliable Drive System for Medical Ultrasound Imaging

By:

Sarah Abourakty, Sarah Ames, Aarthee Baskaran, Shipra Trivedi

Advisor:

Zachary Leonard
Rivanna Medical

Word Count: 3528
Figure(s): 8
Table(s): 0
Equation(s): 0
Supplement(s):0
Reference(s): 17

Approved Zach Leonard Date May 6, 2022

Development of a Reliable Drive System for Medical Ultrasound Imaging

Sarah Abourakty[a], Sarah Ames[b], Aarthee Baskaran[c], Shipra Trivedi[d]

[a] sa2pp@virginia.edu
[b] sha3qk@virginia.edu
[c] aab2ua@virginia.edu
[d] st2cp@virginia.edu

Abstract

Ultrasound is becoming an increasingly used technology to provide guidance for epidural injections[1]. Ultrasound imaging allows physicians and technicians to view relevant anatomy before and during an injection procedure, increasing the accuracy of the needle placement. Ultrasound provides advantages over unguided injections in that ultrasound imaging capability allows the physician to track the needle placement, and provides advantages over CT and fluoroscopy imaging in that ultrasound is more affordable for patients and hospitals, more accessible to hospitals in remote areas and developing countries, and that ultrasound doesn't expose the patient to radiation. The goal of this capstone project was to assist Rivanna Medical Inc. in the development of a new ultrasound probe designed for epidural injections. Development included choosing an appropriate motor and actuator setup, developing a flex circuit compression and extension (flex management) system, performing feasibility testing of the flex management system, performing characterization testing of noise and force produced by the device, and to design test fixtures as needed. Resistance measurements obtained during flex management testing indicated function of the flex circuit until the anticipated lifespan of the device and noise testing demonstrated that the fixture generated sufficiently low noise levels (less than 60 dB). Force testing was conducted with the probe oriented for three patient positions (prone, lateral decubitus, and seated); the prone position resulted in the lowest current draw by the motor, while the lateral decubitus position resulted in the highest current draw. Together, these elements of the capstone project aided the team at Rivanna Medical to develop a reliable drive system.

Keywords: Ultrasound, Epidural, Imaging, Feasibility Testing, Characterization Testing

Introduction

Epidural steroid injections are commonly performed medical procedures, often for the treatment of chronic pain, pre- and post-operative pain management, and regional anesthesia[2]. Injections are performed either unguided or guided via a combination of fluoroscopy and computerized tomography (CTF) scans, performed in an interventional radiology suite[3]. Many injections are performed unguided by a physician as this method is the least expensive and most accessible option, in that only the physician and needle equipment are needed. When unguided, the "loss of resistance" technique is used to perform the injection. This technique states that the needle will first face resistance as it punctures through the ligamentum flavum and interspinous ligament and then will lose resistance as the needle enters the epidural space if the injection was done in the correct area[4]. While physicians are highly trained in this technique high failure rates are still common, such as a failure rate of up to 38% in caudal injections[5]. Improperly-placed injections which are not caught prevent medication from reaching its target, preventing the desired pain relief. Improperly placed injections which are caught are redone but this results in increased patient pain and discomfort[1].

Available alternatives to unguided injections are to use fluoroscopy and CT (CTF) imaging, as provided in an interventional radiology suite. In this technique, the spine is first imaged with CTF to locate an acceptable area of puncture and best angle for the needle to minimize patient discomfort[6]. Once the spot is chosen, the needle is slowly inserted, tracking its progress with CTF scans as it punctures the ligamentum flavum and is further inserted into the epidural space. Once in the epidural space, a

contrast medium is injected. The contrast medium should have a linear appearance if in the epidural space but if not, a needle replacement may be needed. Only once the needle is confirmed to be properly placed is the steroid medication injected.

While the benefits of CTF are highly desirable for both patient comfort and procedure effectiveness, the drawbacks from it leave a need for an alternative imaging technology. The drawbacks of CTF are that it is comparatively expensive, it exposes patients to radiation, and that it is not accessible to hospitals in low-income areas, remote areas, or in developing countries. In 2018, a cervical spinal epidural steroid injection without fluoroscopy (assumed without CTF) would cost around $300 but with fluoroscopy would cost over $450[7]. Similarly, a lumbar spinal injection would cost approximately $285 without fluoroscopy but $450 with fluoroscopy. This $150 and $165 increase to add fluoroscopy for cervical and lumbar injections respectively adds burden to patients, particularly for those receiving periodic injections for chronic pain. For an individual receiving quarterly cervical spinal injections, the use of fluoroscopy would add approximately $600 to their annual medical bill. Even if the extra cost is worth the assurance of a successful procedure, a cheaper guidance option is desirable to make guidance more affordable and accessible.

The cost of an interventional radiology suite prohibits its use in all hospitals. Building an interventional radiology suite is an investment often costing upward of $2.5 million[7]. This puts the technology out of the scope of less wealthy hospitals, often located in rural or low-income areas. Thus, doctors and patients in these areas are more likely to rely on unguided injections as their only technique.

The real-time functionality of CTF allows physicians to actively track the path of the needle, although this comes at a cost. Fluoroscopy provides the real-time functionality but is made more powerful when combined with CT technology[8]. Because CTF uses approximately 20x the x-ray tube current of traditional fluoroscopy, has greater x-ray potential than traditional fluoroscopy, and because the addition of CT x-ray beam is highly filtered and rotates, CTF exposes the patient to higher levels of radiation than traditional fluoroscopy.

The combined downsides of high cost, inaccessibility, and radiation exposure create a need for an alternative real-time guidance technology. That's where ultrasound comes in. Medical ultrasound works by using a pulse-echo transducer to generate an electrical pulse, sending that pulse through piezoelectric crystals which convert the electrical pulse to a mechanical pulse (sound wave), sending the sound wave into the body where it is reflected off a solid surface and sent back into the transducer lens[9]. The piezoelectric crystals convert the sound wave back into an electrical pulse which is picked up by the transducer. By collecting data from many pulses, a physician or technician can diagram a patient's internal anatomy for diagnostic and surgical purposes.

Ultrasound is a safe and generally more accessible alternative to x-ray and MRI imaging. It is already the standard for abdominal and pelvic imaging, in order to protect reproductive organs from radiation, but is becoming more common for other fields such as cardiovascular and tissue mass imaging[10]. Medical ultrasound generally provides a more pleasant patient experience since most ultrasound transducers are handheld or easily mobile, allowing the patient flexibility in how they sit or stand during imaging, as opposed to x-rays and MRI machines which require specific, strict patient orientation. In terms of epidural injections, medical ultrasound provides guidance for needle insertion while preventing radiation exposure and is a relatively accessible and affordable option.

Rivanna Medical Inc. is developing a new ultrasound device designed to provide guidance for epidural injections. They currently have one device on the market, the Accuro (Figure 1). The Accuro is a pocket-sized device containing a probe and a rotatable touchscreen which provides imaging guidance for lumbar and thoracic epidural injections[11]. Physicians are able to produce real-time ultrasound imaging of both the spinal bone and surrounding tissue with the Accuro, providing an imaging alternative without the drawbacks of CTF as discussed. Results from clinical studies with the Accuro have indicated an increase in first attempt success rates, a reduction in needle passes, a reduction in placement times, and patient satisfaction with pain control[12]. Proprietary ultrasound technology (software and hardware) makes the Accuro successful when used for both non-obese and obese patients, an advantage over most existing ultrasound technology which struggles with obese patients and those with difficult anatomy. Successful market performance of the Accuro has led to funding for a next generation version of the device which is currently in development.

Fig. 1. Rivanna Medical's Accuro Device[13]

The role of this capstone project was to assist Rivanna Medical in the development of their next generation Accuro. Most advantages of the next version are currently proprietary information but of note is that the device will be configured such that the attending physician can have two hands available to perform the injection. The new device contains a linear drive system which translates the ultrasound transducer along a linear path. The role of the capstone team was to choose an appropriate actuator, develop a flex circuit extension and compression (flex management) system, perform feasibility testing of the flex management system, perform characterization testing of the noise produced by the device and the force needed to drive the motor, as well as to design and 3D print test fixtures as needed.

The first tasks were to choose an actuator setup and to develop the flex management system. The actuator would need to move back and forth across a specified distance in incremental movements and would be compared to an existing actuator setup. The requirements of the flex management system were that the flex circuit would be able to move with the ultrasound array, extending to nearly its maximum length when the array moved to the distal end of the device, and compressing to a shorter length when the array moved back, proximal to the motor. Once these subsystems were developed, testing methods were developed to characterize and ensure reliability of the systems.

Results

Actuator Selection

The first deliverable involved the comparison of an existing motor driver to a new motor driver system configured by the team. The new motor driver system was controlled with a program to drive the array back and forth across a 75 mm distance in 2 mm increments. After hardwiring a new circuit to control a brushless DC (BLDC) motor and comparing its performance to an existing configuration, the team found the existing motor driver to be the optimal control hardware for future testing purposes. The existing motor driver allowed for magnetic position sensor control, which would allow for more accurate control of the motor throughout the product's usage.

Flex Management

After experimenting with different mechanisms, the team decided to pursue a rack and pinion mechanism to accommodate the variable length of the flex circuit throughout the actuator travel range. This system became known as the flex management system. A spool was first prototyped out of foam, and consisted of a cylindrical vessel that had a rectangular cut-out sized for the flex circuit. Once the proof of concept for coiling was established, the spool was 3D printed. This spool was then attached to a gear at the end opposite the cutout. The gear fit between two gear racks, and the upper rack was propelled forwards and backwards based on the movement of the motor. This final flex management system coiled the flex circuit in the center of the device, and expanded to the maximum length as defined by the device requirements. This design was implemented into the device, and was tested to prove reliability, as highlighted in the next section.

Testing

Three separate testing protocols were generated to assess the impact of the flex management system on the trace resistances of the flex circuit, the noise and force levels, and the acoustic coupling between the array and the lens. After all testing protocols were finalized, the flex management and force and noise testing were executed. Three fixture orientations are mentioned throughout testing: prone, lateral decubitus, and seated. In the prone position, the patient lies on their stomach (Figure 2a). In the lateral decubitus position, the patient lies on their side (Figure 2b). In the seated position, the patient is sitting in an upright position with their back straight (Figure 2c).

Figure 2a

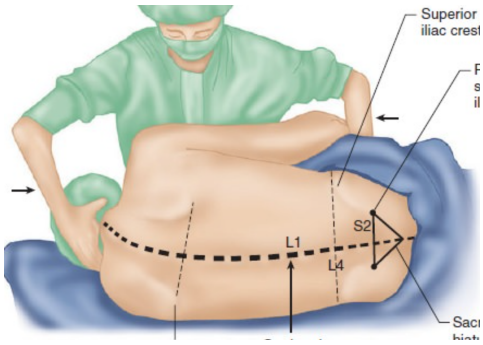

Figure 2b

Figure 2c

Fig. 2a-c. Patient in prone[14] (a), lateral decubitus[15] (b), and seated position[16]

Flex Management Testing

The objective of the flex management testing was to evaluate the reliability of the flex circuit spooling mechanism over the device lifespan. Throughout the flex testing, the rack and pinion design was monitored to ensure consistent coiling and uncoiling of the flex circuit. The flex testing was conducted in the three different orientations that reflect the device's clinical implementation. The prone orientation places the bottom of the device parallel to the ground with the array traveling horizontally, the lateral decubitus orientation places the bottom of the device perpendicular to the ground with the array traveling horizontally, and the seated orientation places the bottom of the device perpendicular to the ground, with the array traveling vertically. Flex management testing was also performed in the absence and presence of silicone oil, which was the primary coupling fluid used throughout testing. At incremental cycles, the flex circuit was removed from the fixture, after which the integrity of the flex circuit was evaluated through measuring the resistance of the flex traces. Data from the trace resistances was analyzed by examining trends in resistance over time to evaluate the lifespan of the flex circuit.

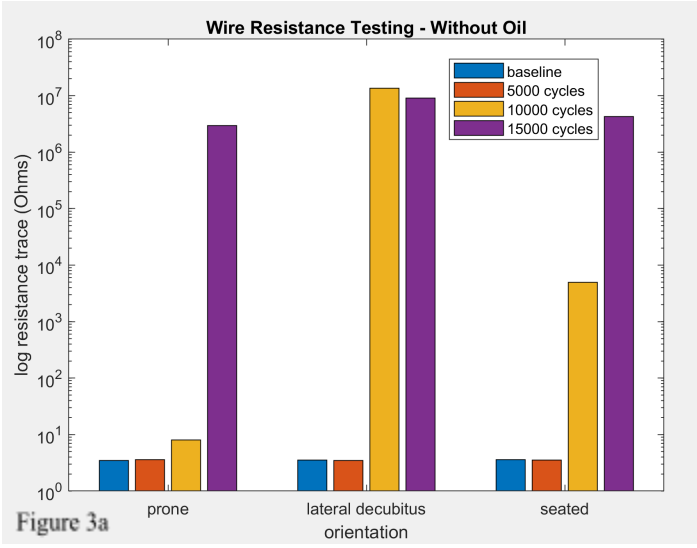

Figure 3a

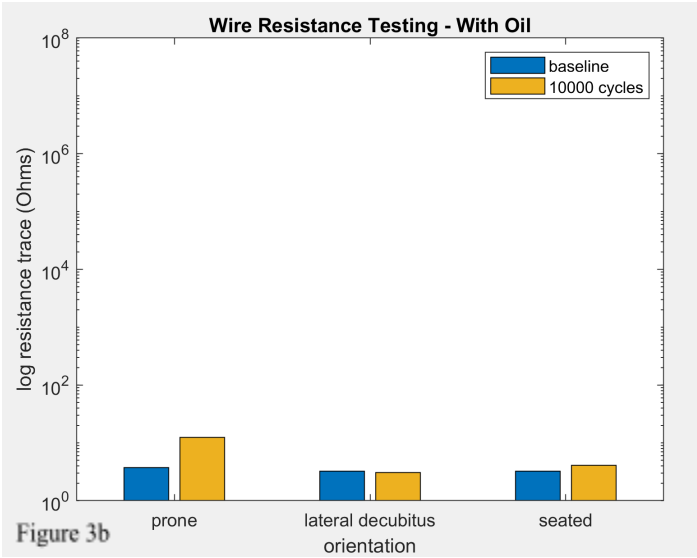

Figure 3b

Fig. 3a-b. Preliminary testing without oil indicated no wire failure up until 10,000-15,000 cycles (a). Testing in oil up to 10,000 cycles indicated little to no wire failure (b).

For testing performed with no oil (acoustic coupling fluid), measurements were taken every 5,000 cycles from the baseline to 15,000 cycles (Figure 3a). No data indicated that any traces of the flex circuit broke by the 5,000 cycle mark, as would be indicated by a sharp increase in the resistance measurement. By 10,000 cycles for both the lateral decubitus and seated positions enough wires had

broken or been damaged that the resulting increased resistance values strongly increased the average. The log transform of all values was taken before plotting, since resistance values ranged from Ohms to Megaohms.

Testing in air confirmed the estimate that the device lifecycle would be approximately 10,000 cycles, so trace resistance measurements in oil were limited to baseline and at 10,000 cycles (Figure 3b). While the drive system visually and audibly had to work harder, there was no indication that any traces of the flex circuit broke within the 10,000 cycle range for any orientation, although one trace for the prone testing may have been slightly damaged as there was one trace with a resistance value in the Kohm scale.

Noise Testing

Testing was performed in prone, lateral decubitus, and seated orientations. Noise (dB) readings were measured both before the fixture was run (baseline) and during operation of the device.

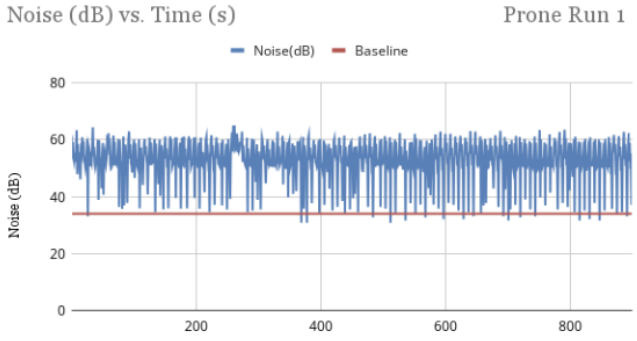

Figure 4a

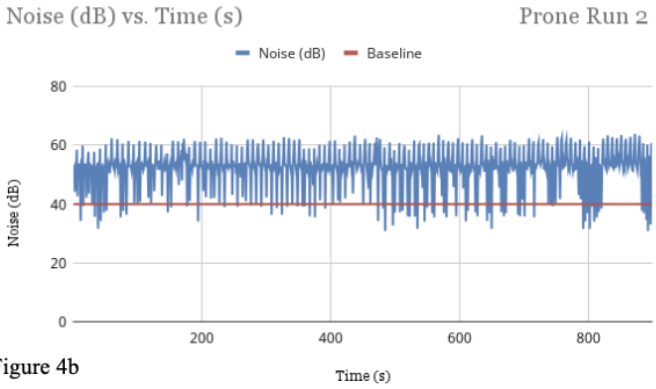

Figure 4b

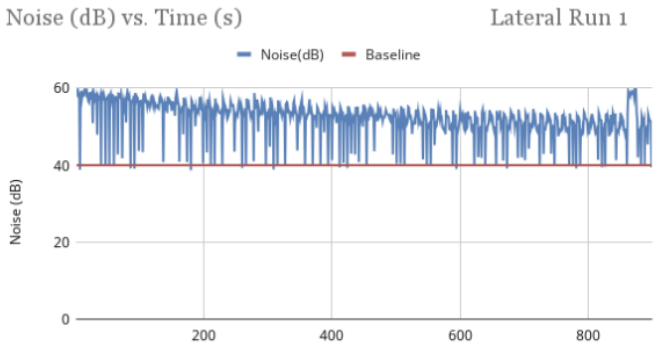

Figure 4c

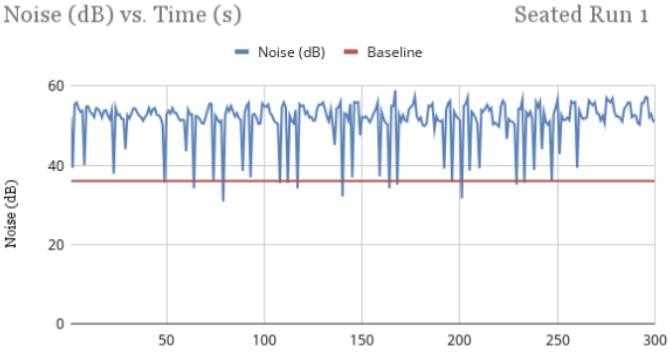

Figure 4d

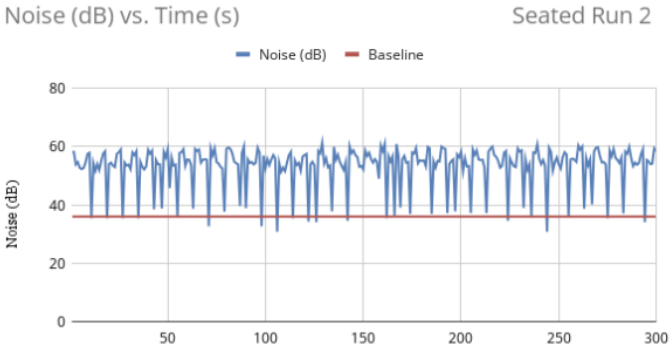

Figure 4e

Fig. 4a-e. Noise (dB) data plotted against time (s). Prone and lateral runs (a-c) were performed for 15 minutes in intervals of 1 second while seated (d-e) were performed for 5 minutes with the same interval. Baselines were plotted in red for each run.

Avg. noise (dB)		
Prone	**Lateral**	Seated
54.85	**53.38**	54.05
Peak noise (dB)		
Prone	**Lateral**	Seated
64.5	**60**	60.1

Fig. 5. Data metrics were pulled from the noise data: average noise while the fixture was operating and max noise generated.

The decibel readings for prone, lateral decubitus, and seated are displayed in Figure 4a-e. The average baseline readings for prone, lateral decubitus, and seated were 37, 40, and 36 dB, respectively.

Force Testing

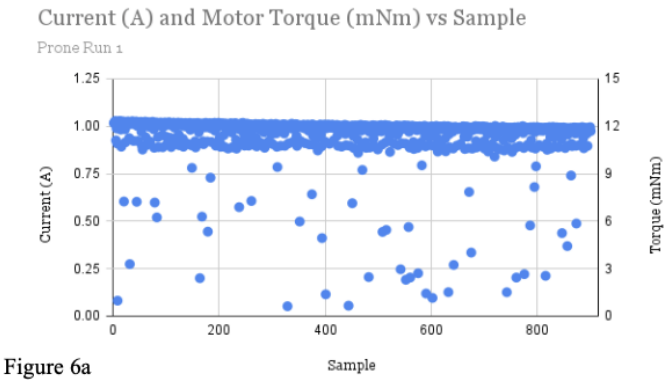

Figure 6a

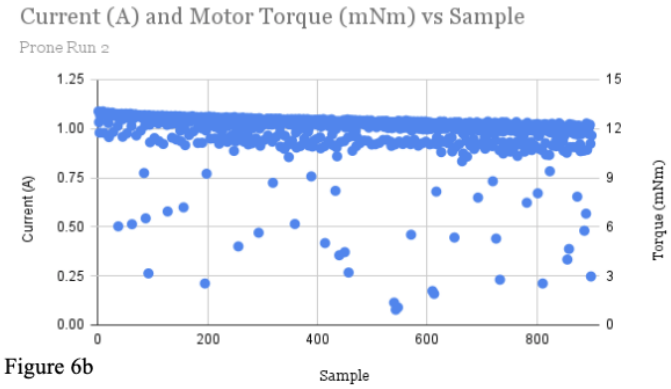

Figure 6b

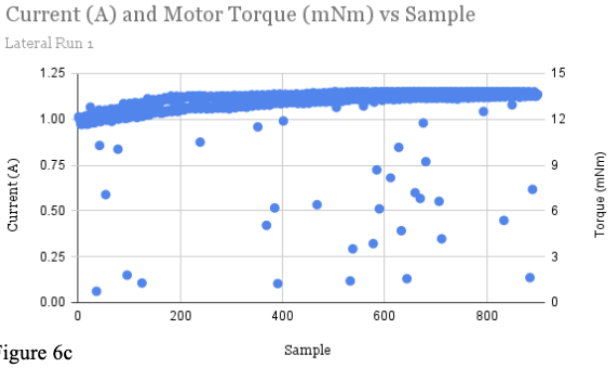

Figure 6c

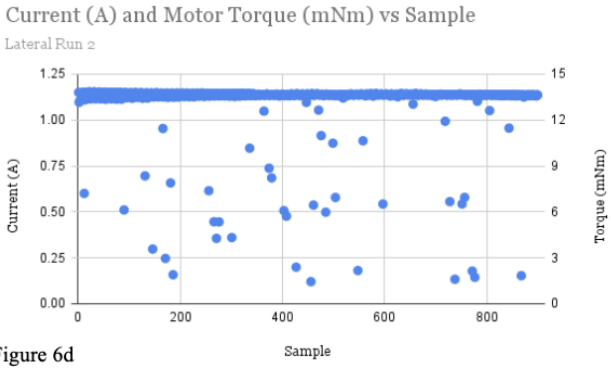

Figure 6d

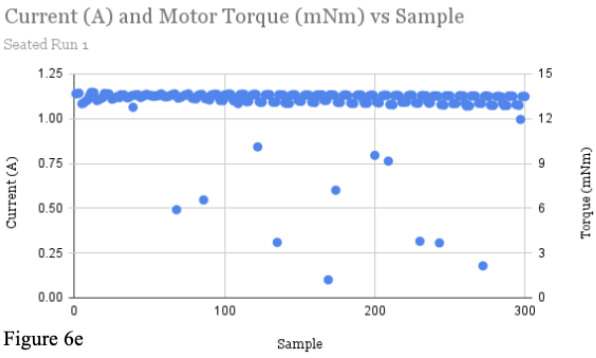

Figure 6e

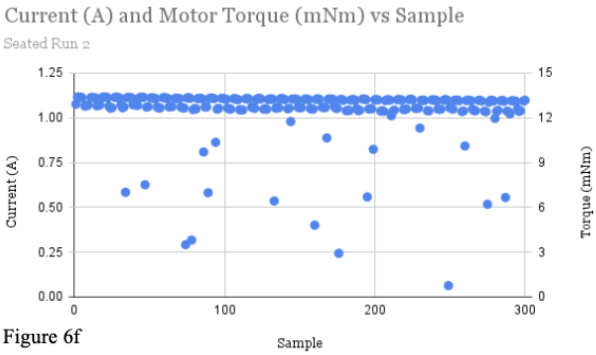

Figure 6f

Fig. 6a-f. Current (A) and torque (mNm) data were plotted against samples. 900 samples were collected of prone and lateral runs (a-d) while 300 samples were

collected for seated (e-f). The torque was calculated using a conversion factor of 12.

Avg. current (A)		
Prone	Lateral	Seated
0.97	1.10	1.07
Max current (A)		
Prone	Lateral	Seated
1.06	1.15	1.14

Fig. 7. Average current during operation and max current generated were calculated for all orientations.

The current measured in the force testing, in all orientations, is displayed in Figure 6a-f. The range of average currents was between 0.97 A and 1.10 A.

Acoustic Coupling

Protocols to test the acoustic coupling of the device were generated. The main variable in the documentation was the viscosity of the coupling fluid, silicone oil, which included 50, 1000, and 3000 cSt oils. The objective behind this testing was to examine the size and quantity of air bubbles when the device ran with each type of oil, and select the oil that had the least amount of air bubbles based on number of bubbles per cycle and size. This would help determine how well the acoustic coupling between the lens and the array was. The acoustic coupling testing was never implemented due to a change in resources and change of scope for the project.

Discussion

Flex Management Testing Results

Data from the flex management testing both with and without the acoustic coupling oil was promising for confirming that the flex management system is an acceptable method for compressing and extending the flex circuit. While the data for the testing without oil indicated some damage to traces of the flex circuit, as seen by increased resistance values (Figure 3a), the raw data indicated that only some traces increased in resistance, while others remained at the same or similar resistance values as their baseline. In this case, if some traces serve as backup in case of a full break, it can be presumed that the flex circuit would make it through the entire lifecycle of the device.

More important is the data collected with oil, since the final product will contain acoustic coupling fluid such as the oil. In this scenario, since none of the tested wires indicate significant break or damage, there is greater confidence that running the flex management system in oil will not damage the flex circuit and will properly extend and compress the flex circuit as needed through the device lifetime.

Noise Results

Results from the noise testing demonstrated that the noise generated by the fixture and its subcomponents are reliable. A max reading of 60 dB was set as an acceptance criterion to ensure the device will not cause any auditory discomfort for the patient or physician. According to the American Academy of Audiology, 60 dB is categorized as a moderate level of noise such as the level of a normal conversation or dishwasher[17]. Noise of that level will not cause any damage. Results from the tests showed that the average noise, in all orientations, was within this range (Figure 5). Additionally, the prone orientation had the highest average noise generated of 54.85 dB while lateral decubitus had the lowest with 53.38 dB. The results for lateral decubitus didn't follow the typical noise pattern as Figure 4c shows a slight decline; this could be due to changes in ambient noise during the test. The peak noise was around 60 dB, indicating that the noise factor of the fixture is reliable.

Force Results

The average current and torque measurements ranged from 0.97 A to 1.10 A and 11.64 mNm to 13.2 mNm, respectively (Figure 7). These readings were approximately 20 times higher than results from preliminary tests conducted in the absence of oil and indicated that the drag induced on the motor by the oil caused a substantial increase in power draw to reach the same output speed. Therefore, future testing is recommended to determine if drag can be reduced by a lower viscosity oil. Additionally, lateral decubitus resulted in the highest average current with 1.10 A while prone had the lowest average current with 0.97 A. This trend is also reflected in the max current data; the max current for lateral decubitus was 1.15A and the max current for prone was 1.06 A. This indicates that the prone orientation will result in the least work done by the motor and will draw the least power over time. However, this trend in data doesn't correspond with the trend seen in noise testing as the prone produced the most noise.

Limitations

One limitation in this study revolved around the device's performance once submerged in silicone oil. There were clear differences in running, monitoring, and maintaining the device during testing in the absence and presence of oil. Over the course of the tests, the fixture would require manual intervention to fix issues with the motor, magnetic strip, and the flex management system, resulting in unanticipated delays. Mechanical parts of the fixture were also replaced and reassembled in between tests to ensure optimal function of the device. Additionally, there were different mechanical issues depending on the orientation of testing, which would require manual intervention and correction. Another limitation resulted from running the device for extended periods of time, which would cause weathering of various components and require additional time to replace said components.

Further limitations stemmed from the acoustic coupling system and testing. Due to supply chain issues, the beamformer which was required to generate the ultrasound images could not be obtained, which led the team to develop a different method of qualitatively assessing the acoustic coupling images. However, this testing was ultimately not completed and the team shifted to conducting flex reliability testing followed by force and noise testing. This was anticipated, and the team focused more on accomplishing the other tests as they were determined more important for the project.

Future Steps

Future work stemming from this study should focus on several areas of study. First, the proof-of-concept flex management system could be modified to be compatible with future iterations of the overall device. An alternative solution would be to improve the flex management system to accommodate for future design changes. Should the flex management system continue to be incorporated into future iterations of the device, design for manufacturing considerations will need to be taken into account. Many difficulties with small parts of the flex management system were due to improper tolerancing either due to inaccuracies in the 3D printing or not being able to order an off-the-shelf part with ideal dimensions. When developing the subsystem further, final materials and manufacturing methods will need to be chosen. The metal lead screw may remain the same since it was already specifically ordered for the device but all plastic parts including the pinion gear, gear racks, gears on the motor, and spool will need final designs. It may be easiest to mold or machine some of the parts once final dimensions are determined, in order to increase accuracy from 3D printing and off-the-shelf vendors. Once final parts are designed, standardization of the manufacturing process will need to take place as well.

An additional future step pertains to the acoustic coupling dosing system, which was originally within the scope of the project and the testing protocol, but fell out of the scope of the study due to the fixture's complete submersion in silicone oil. However, acoustic coupling between the array and the lens can be a future area of study to determine the optimal form of coupling fluid delivery.

Materials and Methods

Actuator Development and Selection

In order to test different motor driver systems to optimize the overall testing process, a new motor driver system was configured and compared to an existing motor controller. Both motor controllers were developed to control a brushless DC (BLDC) motor. The new motor driver system was wired based on the datasheet provided by the motor driver manufacturer. After the initial circuit was developed, a program was developed using the motor driver's proprietary software to have the array move back and forth across a 75 mm distance in order to test the efficacy of the new system. However, due to an error in the datasheet, two pins for the board connector were mislabelled and wired incorrectly. This incorrect configuration resulted in several issues with the motor driver's performance, which mainly included overheating of the motor. Different combinations of wiring were tested to find the optimal configuration that prevented motor overheating. After the final correct circuit was determined, a program was developed to move the array back and forth across a 75 mm in 2 mm increments. The two systems were compared based on the most accurate array positioning and their compatibility with magnetic position sensor control.

Flex Management Design

The flex management system was designed to guide the movements of a flex circuit as it moves with the ultrasound array. Based on the size of the device body, the flex circuit had to be able to extend to the full length of array travel at the distal end of the device, as well as compress to fit behind the array at the retracted position, when the array was proximal to the motor. Dimensions were based on the internal dimensions of the body and the predetermined distance of array travel. The initial proposal was to fold the

flex circuit in an accordion style, but when unable to design components to facilitate such motion, the alternative of coiling was chosen. Coiling the flex circuit from either end was not possible due to solid connectors at both ends so the system was designed to coil the flex from the middle. A cylindrical rod was designed to roll the flex around which has a slit in the middle to secure the middle of the flex.

The rotational motion of the cylinder had to be externally induced since the cylinder motion is separate from the movement of the array which is controlled by the actuator. Originally, two constant force springs were wrapped around the cylinder ends with the flat ends connecting to the trolley responsible for array motion. No configuration of constant force springs ended up working either due to size incompatibility or incompatible strength levels. Ultimately no configurations produced the rotational motion of the cylinder needed to wrap up the flex. The next design choice was to develop a gear rack and pinion system, with the pinion gear on one end of the cylinder, and a gear rack both above and below the pinion. The bottom gear rack is stationary and embedded into the base of the device. The top gear back is attached to the trolley which moves the array, and thus provides the same range of motion to the rolling cylinder as is provided to the trolley and array. The mobility of the top gear rack provides the needed rotational motion to move the array and flex circuit together. Proof of concept testing was performed to ensure the functionality of the design. Adjustments were made to the size and shape of the cylinder and gear rack configuration but the overall subsystem remained as the final design choice and was used in further characterization and reliability testing.

The flex circuit, or flexible printed circuit, is a custom made circuit board, specifically designed for the new ultrasound probe, which contains copper traces. The flex circuit needed to be compressed in an effective manner, when the traces were not damaged, and the existing motor could be used to drive the force of the compression system. In the first iteration of the design, constant force springs were proposed to coil the circuit in the designated space, relying on the extension of the spring to resist the loading force and coil the circuit. This model proved to be faulty, as the constant force springs were not reliable and would easily deform after repeated use. The springs were also not easily implemented into the device and posed room for failure.

Flex Management Testing

The flex management testing was performed to determine the effect of the flex management subsystem on the flex circuit lifespan. The condition of the electrical traces were evaluated after the device operated for its expected lifespan of 30,000 cycles. At various intervals, 19 pins were measured and the resistance for the corresponding trace was recorded. A Keysight U1233A Multimeter was used to measure trace resistance. Additional materials needed for this test were the flex circuit, silicone oil with a viscosity of 1000 cSt, and resistance measurement breakout boards. The fixture was run in three different orientations: seated, prone, and lateral decubitus. All three orientations were tested both with and without oil. During testing without oil, resistance measurements were taken every 5,000 cycles starting from baseline to 30,000. Testing with oil required taking measurements at baseline and 10,000 cycles. While resistance measurements were primarily taken after removing the flex circuit from the device, they were also taken with the flex in the device when the array was at both ends of the device as well as in the middle at approximately 10,000 and 15,000 cycles.

Fig. 8. Setup for noise and force testing using the decibel meter, multimeter and 12 V power source.

Force and Noise Testing

Force and noise levels were measured during several runs of the device in the prone, seated, and lateral decubitus positions, with the device filled with silicone oil. The noise levels were measured in decibels, and the force was measured using current supplied to the motor (in amperes) as a proxy for force measurements. The torque, in mNm, was calculated using a conversion factor of 12. The device was placed on a test fixture, which allowed for its position to be elevated and in close proximity to the Decibel Meter,

which was placed on a connecting fixture (Figure 8). The decibel meter was then connected to the Noise Logger Communication Tools Software on a laptop. Simultaneously, the power supply and motor driver were connected to the Keysight U1233A Multimeter. The multimeter was connected to the Agilent GUI Data Logger Software on the same laptop as for the decibel meter. Data collection for force and noise was conducted simultaneously for approximately 15 minutes, which allowed for a collection of 900 samples of noise and current measurements.

End Matter

Author Contributions and Notes

The authors declare no conflict of interest.

Acknowledgments

We would like to thank our advisor, Zachary Leonard, and the team at Rivanna Medical for their support and guidance in this capstone project. We would also like to thank the teaching team of the biomedical engineering capstone design course at the University of Virginia.

References

1. Karmakar MK, Li X, Ho AMH, Kwok WH, Chui PT. Real-time ultrasound-guided paramedian epidural access: evaluation of a novel in-plane technique. *Br J Anaesth*. 2009;102(6):845-854. doi:10.1093/bja/aep079https://audiology-web.s3.amazonaws.com/migrated/NoiseChart_Poster-%208.5x11.pdf_5399b289427535.32730330.pdf
2. Shaw BA, Watson TC, Merzel DI, Gerardi JA, Birek A. The Safety of Continuous Epidural Infusion for Postoperative Analgesia in Pediatric Spine Surgery. *J Pediatr Orthop*. 1996;16(3):374-377.
3. Lee L, DeCara JM. Point-of-Care Ultrasound. *Curr Cardiol Rep*. 2020;22(11):149. doi:10.1007/s11886-020-01394-y
4. Dhansura T, Shaikh T, Maadoo M, Chittalwala F. Identification of the epidural space-loss of resistance to saline: An inexpensive modification. *Indian J Anaesth*. 2015;59(10):677-679. doi:10.4103/0019-5049.167483
5. Naidoo K, Alazzawi S, Montgomery A. The Use of Contrast in Caudal Epidural Injections under Image Intensifier Guidance: Is It Necessary? *Clin Orthop Surg*. 2017;9(2):190-192. doi:10.4055/cios.2017.9.2.190
6. Wagner AL. CT Fluoroscopy–Guided Epidural Injections: Technique and Results. *Am J Neuroradiol*. 2004;25(10):1821-1823.
7. Smart Planning for Successful Interventional Radiology Suites. Accessed May 2, 2022. https://blog.array-architects.com/kc/smart-planning-for-a-successful-interventional-radiology-suite
8. Nickoloff EL, Khandji A, Dutta A. RADIATION DOSES DURING CT FLUOROSCOPY. *Health Phys*. 2000;79(6):675-681.
9. The ultrasound transducer. ECG & ECHO. Accessed May 2, 2022. https://ecgwaves.com/topic/the-ultrasound-transmitter-probe/
10. Ultrasound instead of CT. :5.
11. Accuro-IFU-735-00005-RS-Eng.pdf. Accessed May 2, 2022. https://rivannamedical.com/wp-content/uploads/2020/03/Accuro-IFU-735-00005-RS-Eng.pdf
12. Accuro's automated spinal navigation technology is clinically proven | RIVANNA. Published December 8, 2017. Accessed May 2, 2022. https://rivannamedical.com/clinical-value/
13. 736-00022Rev.C-Accuro-image-guidance-brochure-pages.pdf. Accessed May 4, 2022. https://rivannamedical.com/wp-content/uploads/2021/01/736-00022Rev.C-Accuro-image-guidance-brochure-pages.pdf
14. Themes UFO. Interlaminar Epidural Injection. Anesthesia Key. Published May 26, 2016. Accessed May 2, 2022. https://aneskey.com/interlaminar-epidural-injection/
15. Caudal Anesthesia. Accessed May 2, 2022. https://www.brainkart.com/article/Caudal-Anesthesia_27224/
16. 226 Epidural Stock Photos, Pictures & Royalty-Free Images - iStock. Accessed May 2, 2022. https://www.istockphoto.com/photos/epidural
17. NoiseChart_Poster-8.5x11.pdf_5399b289427535.32730330.pdf. Accessed May 2, 2022. https://audiology-web.s3.amazonaws.com/migrated/NoiseChart_Poster-%208.5x11.pdf_5399b289427535.32730330.pdf